Soft Matter

RSC Publishing

PAPER

Mechanical stretch for tunable wetting from topological PDMS film

Cite this: *Soft Matter*, 2013, **9**, 4236

Shuai Zhao,[a] Hong Xia,*[acd] Dong Wu,[a] Chao Lv,[a] Qi-Dai Chen,[a] Katsuhiko Ariga,[cd] Lian-Qing Liu[e] and Hong-Bo Sun*[ab]

Received 16th December 2012
Accepted 15th February 2013

DOI: 10.1039/c3sm27871a

www.rsc.org/softmatter

In this paper, we report a mechanical stretch method for tunable wetting from elastic topologically grooved poly(dimethysiloxane) films. The mechanical strain was applied to elongate the film along two orthogonal directions, perpendicular and parallel to the grooves. Along with the increase of mechanical strain, the primary anisotropic wetting of the films was turned into isotropic or a larger degree of anisotropy depending on the stretching direction. The roughness factor as well as the energetic barrier are responsible for the wetting tuning. Effects of the height and period on tunable wetting were investigated, and multiple-cycle reversible switching between anisotropic and isotropic many times was achieved.

Introduction

Smart surfaces with controllable transitions of surface wettability under external stimuli have received great attention in recent years due to their special use in biological applications, microfluidics, and self-cleaning materials.[1–6] Upon surrounding environmental variations the surface composition and/or morphology of stimuli-sensitive materials is altered, which can adjust surface wetting behavior. Many kinds of external stimuli, such as temperature,[7,8] pH,[9] UV light,[10,11] solvent,[12] electrochemical potential,[13–15] or combinations of two or more of the above stimuli[16] were used to control the wettability of the smart surfaces. These tuning methods of surrounding stimuli greatly contributed to refined control of surface wettability. For practical applications, especially biological species should be affected under rigorous conditions, such as UV irradiation, temperature change, or addition of chemical substances. Therefore, controllable adjusting of surface wettability using general mild stimuli is necessary. Mechanical strain is a simple, facile, safe, environmentally friendly, and biocompatible stimulus method to tune surface wettability. Zhang *et al.* reported an involved study in which biaxial extending and unloading was applied to an elastic polyamide film with a triangular net-like structure, and a reversible switching between superhydrophobic and superhydrophilic wettability was achieved.[17] In the previous work by some of the current authors, a curvature-driven *in situ* switching between pinned and roll-down superhydrophobic states was proposed.[18] In the work, a poly(dimethysiloxane) (PDMS) surface with a regular array of pillars was prepared, which exhibited curvature-dependent contact angle, adhesion force and sliding angle. Based on this unique switching, an *in situ* "mechanical hand" for no-loss water droplet transportation is proposed. Because anisotropic wetting has attracted wide attention due to potential applications involving microfluids, biomedical devices, and self-cleaning, tunable anisotropic wetting behavior by mechanical stimuli is expected. Various topographical patterned surfaces to govern anisotropic wetting behavior have been obtained by many micro- and nanofabrication techniques.[19–23] Dynamic tuning of anisotropic wetting on surfaces or switching between isotropic and anisotropic wetting should provide useful methods for liquid handling, droplet transfer, flow valves, and cell alignment. As a typical correlative investigation Chung *et al.* fabricated anisotropic micro-wrinkled surfaces with sinusoidal profiles by using ultraviolet–ozone treated PDMS elastomer, on which mechanical compression controlled the anisotropic wetting of droplets.[24] The above-mentioned reports indicate that mechanical stimuli are an efficient method to adjust surface wetting, thus more easy-manipulation mechanical stimuli methods are expected to widely tune anisotropic wettability and controllably switch between isotropy and anisotropy. Here, we firstly present a mechanic stretching method combining a topologically flexible film with a microstructure to tune the anisotropic wetting of the surface. Soft lithography combined with photolithography was used to prepare elastic PDMS films with grooved surfaces. Mechanical elongation was applied to the PDMS film along directions

[a]*State Key Laboratory on Integrated Optoelectronics, College of Electronic Science and Engineering, Jilin University, 2699 Qianjin Street, Changchun 130012, China. E-mail: hxia@jlu.edu.cn; hbsun@jlu.edu.cn*

[b]*College of Physics, Jilin University, 119 Jiefang Road, Changchun, 130023, China*

[c]*CREST, Japan Science and Technology Agency, Goban-cho, Tokyo 102-0076, Japan*

[d]*International Center for Materials Nanoarchitectonics (MANA), National Institute for Materials Science (NIMS), 1-1 Namiki 305-0044, Tsukuba, Japan*

[e]*State Key Laboratory of Robotics, Shenyang Institute of Automation, Chinese Academy of Sciences, Shenyang, China*

parallel and perpendicular to the grooves, indicating deformation of topological morphology on the surface of the film. Accordingly, tunable and reversible anisotropic wetting behavior with decreasing and increasing degrees of wetting anisotropy was exhibited by various grooved surfaces with different aspect ratios.

Experimental

Fabrication of grooved PDMS film

We prepared the surfaces using standard clean-room methods. First, glass slides were cleaned with acetone, absolute ethanol, and deionized water. A layer of negative epoxy resin SU-8 2075 (Nano-Micro-Chem Company, American) diluted with cyclopentanone (1 : 1 by mass) was spin-coated at different rotation speeds on glass slides to obtain the needed thicknesses of the resin films. Subsequently, the photoresist was placed in an oven at 95 °C for 30 min to evaporate the solvent. The slides were then removed from the oven and cooled to room temperature. Second, groove arrays in 11 × 11 mm square size with different periods (8, 12, 20, 40, 100 and 200 μm) were fabricated by photolithography. Here a mask aligner ABM/6/350/NUV/DCCD/BSV/M (ABM, Inc., American) was used, the optical power density was 15 mW cm^{-2} and the exposure time was 10 s. After exposure, the sample was baked for 10 min and developed in the SU-8 developer for 1 min. Once the unexposed photoresist was washed off, the grooved SU-8 template was obtained. Third, the regular groove-array template was coated with a layer of PDMS prepolymer, mixing Sylgard 184 (Dow Chemical Co.) in 10 : 1 mass ratio with a curing agent, and cured at 65 °C for 1 h. After being peeled off, grooved flexible PDMS surfaces with thickness of ~1 mm were obtained. Finally, the PDMS surfaces were modified with low energy modification material, fluoroalkylsilane ($CF_3(CF_2)_5$–$CH_2CH_2SiCl_3$), *via* vapor deposition to enhance the hydrophobicity.

Sample characterization

The PDMS film was mounted on a custom-designed strain stage to stretch uniaxially to different ratios (ε, defined as the ratio of elongated length over the original length) along two orthogonal directions parallel and perpendicular to the grooves. Then the contact angle (CA) was measured using a Contact Angle System OCA 20 instrument (DataPhysics Instruments GmbH, Germany) at ambient temperature. A high purity water droplet (~5 μL) was deposited on the sample surface and the static equilibrium CA was measured immediately upon needle removal. The surface topography was imaged with an atomic force microscope (AFM) in tapping mode.

Results and discussion

Tunable wetting by mechanical stretch

The grooved surface PDMS film with size of 11 mm × 11 mm and period of 20 μm was fabricated [Fig. 1(a)], which exhibited excellent elastic recovery at least within the currently used range of strains (100%). A mechanical elongation force along the directions parallel and perpendicular to the grooves was applied

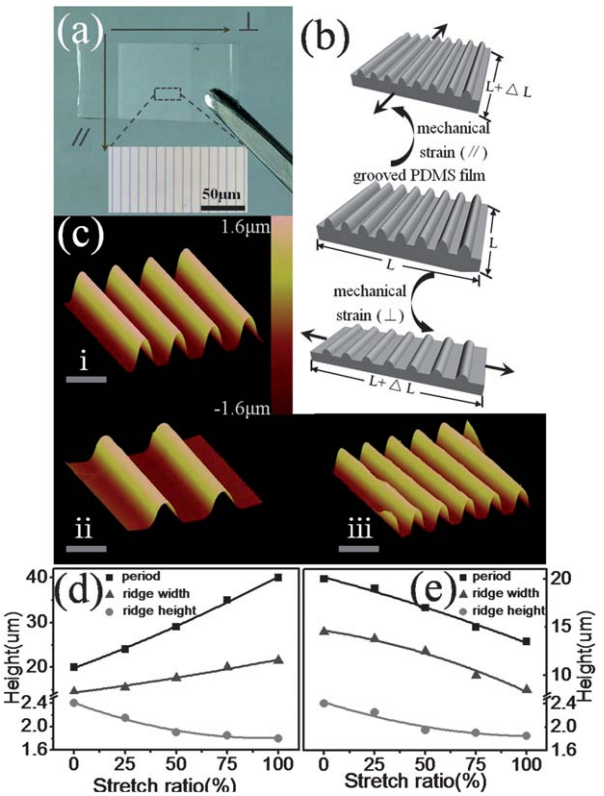

Fig. 1 (a) A digital photograph of this flexible hydrophobic film. (b) Schematic illustration of stretching PDMS films uniaxially to different ratios (ε) by a custom-designed strain stage. (c) AFM images of grooved PDMS surfaces obtained at different stretch ratios, ε = 0% (i), 75% along the direction perpendicular to grooves (ii) and 75% along the direction parallel to grooves (iii). The scale bars represent 10 μm. The groove parameters as a function of mechanical elongation ratio under two orthorhombic directions, perpendicular (d) and parallel (e) to grooves.

to stretch the films. During the stretching process a mechanical deformation of grooved films occurred as illustrated in Fig. 1(b). Upon stretching along the direction perpendicular to the grooves, the period of the grooves became larger, in contrast the period is smaller if the stretching direction is parallel to the grooves. An AFM image [Fig. 1(c-i)] shows the primary grooved surface with an analogue sinusoidal topology with a period of 20 μm and a ridge height about 2.4 μm. From elongation along the direction perpendicular to the grooves the increase of groove period is nearly in direct proportion to the stretching ratio, for example at ε of 75% the groove has a period of 35 μm compared to the unstretched value of 20 μm [Fig. 1(c-ii)], while the ridge height is somewhat decreased to 1.85 μm. From elongation along the direction parallel to the grooves, the period of the grooves is decreasing, and the ridge height is somewhat decreasing with increasing ε, for example a period of 15 μm and a ridge height of 1.9 μm at ε of 75%.

The wetting of a water drop on the grooved surface was investigated at different elongation ratios [Fig. 2]. Without stretching (stretching ratio = 0) the primary surface has anisotropic wetting, the CA was 138° and 120° from perpendicular and parallel direction to the grooves, respectively, while

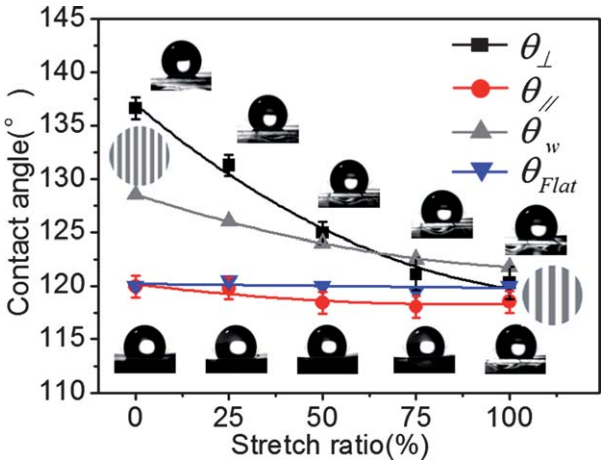

Fig. 2 The relationship between the CA and the stretch ratio. $\theta_{\perp}$ decreased from 138° to 120° as ε increased, while $\theta_{\parallel}$ remained almost constant (~120°). The calculated θ_{w} and θ_{Flat} are also given in contrast. The insets are the bird's-eye view schematic illustrations of the wetted areas.

the CA of a PDMS surface without any topological structure was 120°. The water drop preferentially spreads along rather than perpendicular to the grooves; the increase in hydrophobicity is caused by the enhancement of the surface roughness and higher energy required to overcome the energetic barrier formed at the grooves. Under mechanic stretching along the perpendicular direction to the grooves, CA along the perpendicular direction ($\theta_{\perp}$) remarkably decreased as the strain increased. Upon stretching to 100%, $\theta_{\perp}$ decreased to 120° from the original value of 138°, while the CA along the grooves ($\theta_{\parallel}$) remained almost constant (~119°), indicating an isotropic wetting from anisotropic wetting by mechanical elongation. In contrast, by stretching along the direction parallel to the grooves a larger degree of wetting anisotropy was observed. When $\varepsilon = 100\%$ $\theta_{\perp}$ increased to 142° from the original value of 138°, while the CA along the grooves ($\theta_{\parallel}$) remained almost constant at ~119° [Fig. 4].

Here the liquid fills all of the underlying structural features on the grooved surface with a complete wetting of the liquid–solid interface, and the liquid droplet exists in the Wenzel state. This leads to an increase of the total wetted area with the flat surface. The CA θ_{w} can be estimated using the Wenzel equation: $\cos\theta_{w} = r\cos\theta$, where r is the roughness factor, defined as the ratio of the actually wetted area over the projected area under the droplet; θ is the CA the liquid assumes on the smooth surface.[25] The insets of Fig. 2 are the bird's-eye view schematic illustrations of the wetted areas in the original state and for 100% strain. The wetted area has a near circle-like shape and the diameter (D) is about 1 mm. For typical grooved surfaces (period of 20 μm), the wetted area contains about 50 grooves, and cannot be treated limitlessly. So the roughness factor (r) is calculated by using the formula: $r = 1 + 4Lh/\pi D^2$, where h is the ridge height and L is the total length of the groove edge. The roughness factor gradually decreased from 1.24 to 1.18, 1.13, 1.11, and 1.09 when the strain along the direction perpendicular to the grooves increased from 0% to 25%, 50%, 75% and 100%, respectively. The θ_{w} values (gray line, Fig. 2) were calculated by inserting our experimental parameters into the equation mentioned before. As proved by the curve, the θ_{w} values decrease from 128.5° to 121.8° and agree with the trend of $\theta_{\perp}$. However, the observed $\theta_{\perp}$ values are quite different from the calculated θ_{w}. This result can be understood by considering the anisotropy of the grooved patterns as well as the potential barrier formed at the grooves. When the wetting direction is perpendicular to the grooves, the energy barriers between adjacent grooves supposedly separate the existence of many metastable levels, and therefore the change of the free energy becomes discontinuous. In addition, the droplet is always subject to some external disturbances, and this energy input may assist in overcoming energy barriers up to a certain level. In contrast, by stretching along the direction parallel to the grooves an increased roughness factor is responsible for the larger $\theta_{\perp}$.

The free energy of a water droplet on different stretching ratios was calculated to understand the CA change. The schematic cross sections of the grooved structure and droplet profile are shown in inset (i) of Fig. 3. Corresponding to the constant volume of the water droplet, the profile can be treated as a spherical cap with a constant area.[26] Here, we take the cross section of the grooved structure as a rectangle, a and b stand for the groove spacing and width, respectively, L is the radius of the water droplet. For the Wenzel state, the change in system free energy for a drop changing from a reference position C with drop size (L_{C}) and CA (θ_{C}), to an arbitrary position with L_{D} and θ_{D}, can be expressed as:

$$\Delta F_{C\to D}/\gamma^{la} = \left(\theta_{D}\frac{L_{D}}{\sin\theta_{D}} - \theta_{C}\frac{L_{C}}{\sin\theta_{C}}\right) + \left(\frac{L_{C}-L_{D}}{a+b}\right)(a+b+2h)\cos\theta_{Y} \quad (1)$$

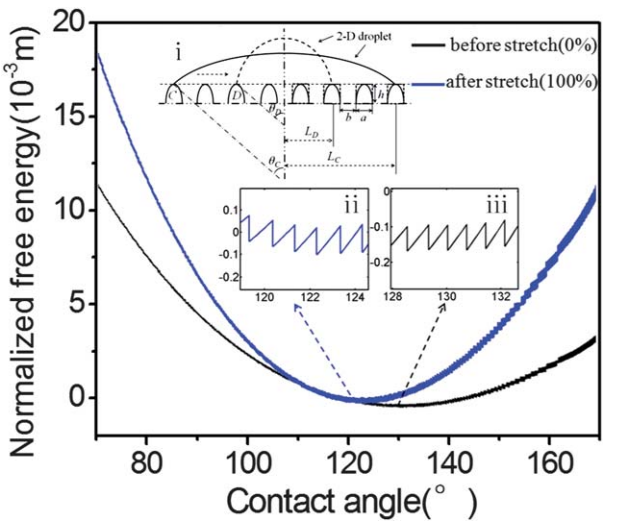

Fig. 3 Normalized system free energy as a function of the CA (intrinsic CA = 120°; $a = b = 10$ μm, $h = 2.4$ μm, black line; $a = b = 20$ μm, $h = 1.8$ μm, blue line). Inset (i) show schematic cross sections of the grooved structure and droplet profile, (ii) and (iii) are enlarged views of segments of the free energy curves.

where γ^{la} is the liquid surface tension and θ_Y is the intrinsic CA of a flat PDMS film. Curves in Fig. 3 exhibit the variation of normalized free energy with CA. The black and blue lines are the unstretched state (period = 20 μm) and double stretched state (period = 40 μm), respectively. Insets (ii) and (iii) show the enlarged views of the minimum sections of the free energy curves, indicating the potential barrier formed at the groove mentioned before. Free energy is a minimum when CA = 130° for the unstretched state, and 121° for the double stretched state, that is, CA will decrease from 130° to 121° upon mechanical stretching. In fact, either a decrease in ridge height or an increased period will decrease the CA in our case.

Adjusting of tunable wetting with grooves of different geometrical parameters

To further clarify the tuning ability of grooved PDMS upon mechanical stretching, $\theta_\perp$ of a set of patterns with different geometrical parameters are presented in Fig. 4. In Fig. 4(a), to study the affect of the groove period on wetting tuning, six patterns were selected, which have the same ridge height of 2.4 μm and different groove periods between 8 μm and 200 μm. Firstly, mechanical elongation along the direction perpendicular to the grooves was applied. For the period of 8 μm, the $\theta_\perp$ changed only by a few degrees (139° to 136°) at 0–100% strain. As the period becomes larger (12–40 μm), original $\theta_\perp$ shows a slight decrease, 138° for 12 μm and 20 μm and 133° for 40 μm, while under strain $\theta_\perp$ reveals a noticeable decrease to 120–125°. When the period is large enough (>100 μm), the $\theta_\perp$ remains almost constant (120° ± 2°) with strain, indicating no obvious tunable wetting. This might be because the energetic barrier formed at the grooves, which prevents water droplets from spreading in the perpendicular direction, becomes more discontinuous when the period increases. In addition, the $\theta_\perp$ of 120° observed for 100% strain for a groove period of 20 μm is smaller than 133° for the unstretched PDMS with a period of 40 μm [Fig. 3(a)]. This is probably attributed to two aspects: firstly, the fluoroalkylsilane density on the stretched surface of PDMS is sparser than on the unstretched original; secondly, the slope degree of sidewalls for the stretched geometry is larger than for the original unstretched geometry although they have the same roughness factor. When the films were stretched along the direction parallel to grooves, the $\theta_\perp$ increased for groove periods of 8–20 μm, but $\theta_\perp$ has no obvious change for periods of 40–200 μm.

For different ridge heights (h), with a constant groove period of 20 μm, the $\theta_\perp$ values are shown as a function of strain of PDMS film [Fig. 4(b)]. For large ridge height (h > 3 μm), $\theta_\perp$ changes a little around 138° (unbroken line) at strain 0–100%. In this case water droplets are in the Cassie state, *i.e.* the droplet rests on the tops of the grooves. The CA θ_c can be estimated by using the Cassie equation: $\cos\theta_c = f(\cos\theta + 1) - 1$. Here f represents the fraction of the liquid interface that is in contact with the solid as compared to the projected surface area. Due to the nearly constant f the $\theta_\perp$ values change a little with increasing strain. For smaller h (<3 μm), water droplets end up in the Wenzel state and the PDMS films show tunable wetting properties (dashed line) upon stretching. Finally, when h is only a few hundred nanometers, the wetting properties (dotted line) become almost the same as for flat PDMS surfaces.

Reversibility and repeatability of tunable wetting by mechanical stretch

According to the excellent elastic recovery of PDMS films, multiple-cycle elongation and releasing was studied to satisfy the demands of practical applications. The PDMS film was gradually stretched from its original length to double length (strain 100%) and kept at that length for an hour. Then the strain was released and the PDMS film came back to its original length. Both $\theta_\perp$ and $\theta_\parallel$ were measured throughout the process [Fig. 5(a)]. First the $\theta_\perp$ decreases from 138° to 120° and then increases from 120° to 138° again, while the $\theta_\parallel$ remains almost unchanged at 119°, indicating a reversible tuning of wetting. The stretching–releasing was repeatedly applied; the PDMS films were cycled between original and 100% strain states. The CA can be reversibly changed many times with no change in responsive wetting. The results show a quick transition as a stretching or releasing lasts only a few minutes. The responsive reversibility remains for a long time without special protection because the PDMS is mechanically and chemically stable.

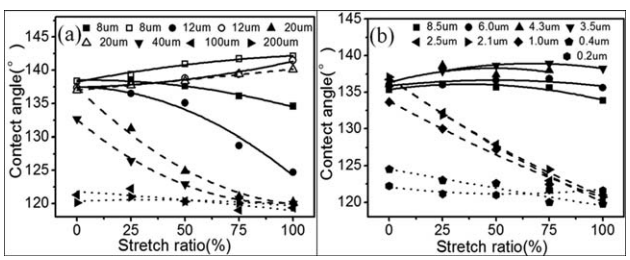

Fig. 4 The relationship between the CA and different groove periods/heights. (a) Groove periods range from 8 μm to 200 μm while h remained constant (~2.4 μm). Lines with hollow symbols stand for stretching along the direction parallel to the grooves while the filled symbols stand for the direction perpendicular to the grooves. (b) Ridge heights range from 0.2 μm to 8.5 μm while the period remained constant (20 μm).

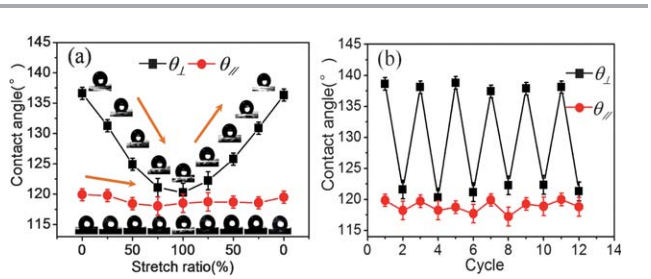

Fig. 5 (a) The reversibility of the wetting properties. The grooved PDMS films showed reversible wettability during loading and unloading in one cycle due to their excellent elasticity. (b) The repeatable switching of the CAs along two directions. The $\theta_\perp$ was tuned between 138° and 120° and the $\theta_\parallel$ showed small fluctuations around 119°.

Conclusion

In conclusion, a mechanical stretching for tuning of anisotropic wetting and switching between anisotropy and isotropy has been proposed for the first time. To demonstrate the stretching tuning, a PDMS surface with grooves was fabricated by photolithography and soft lithography. Experimental results reveal that along with the increase of mechanical strain the primary anisotropic wetting of the surface was turned into isotropic or a larger degree of anisotropy according to the stretching direction, perpendicular or parallel to grooves, respectively. Moreover, the tuning of wetting is reversible and repeatable owing to the robust micro-structure and excellent elasticity of PDMS. This work provides a new insight into smart anisotropic surfaces with tunable wettability for microfluidic devices and liquid transfer, because mechanical stress is a highly versatile stimulus capable of being applied to a wide range of materials.[27]

Acknowledgements

The authors gratefully acknowledge support from the 973 Project (2011CB013005) and the NSFC (Grant nos 61127010, 90923037, and 61137001). We also acknowledge the financial support by the State Key Laboratory of Robotics.

Notes and references

1 S. Daniel, M. K. Chaudhury and J. C. Chen, *Science*, 2001, **291**, 633.
2 F. Xia and L. Jiang, *Adv. Mater.*, 2008, **20**, 2842.
3 B. Chang, A. Shah, I. Routa, H. Lipsanen and Q. Zhou, *Appl. Phys. Lett.*, 2012, **101**, 114105.
4 C. Jiang, Q. Wang and T. Wang, *New J. Chem.*, 2012, **36**, 1641.
5 C. Simão, M. Mas-Torrent, J. Veciana and C. Rovira, *Nano Lett.*, 2011, **11**, 4382.
6 M. He, J. X. Wang, H. L. Li, X. L. Jin, J. J. Wang, B. Q. Liu and Y. L. Song, *Soft Matter*, 2010, **6**, 2396.
7 M. He, H. Li, J. Wang and Y. Song, *Appl. Phys. Lett.*, 2011, **98**, 093118.
8 T. L. Sun, G. Wang, L. Feng, B. Liu, Y. Ma, L. Jiang and D. Zhu, *Angew. Chem., Int. Ed.*, 2004, **43**, 357.
9 E. Stratakis, A. Mateescu, M. Barberoglou, M. Vamvakaki, C. Fotakis and S. H. Anastasiadis, *Chem. Commun.*, 2010, **46**, 4136.
10 H. Cui, G. Z. Yang, Y. Sun and C. X. Wang, *Appl. Phys. Lett.*, 2010, **97**, 183112.
11 H. S. Lim, D. Kwak, D. Y. Lee, S. G. Lee and K. Cho, *J. Am. Chem. Soc.*, 2007, **129**, 4128.
12 X. Wang, G. Qing, L. Jiang, H. Fuchs and T. Sun, *Chem. Commun.*, 2009, 2658.
13 C. Badre and T. Pauporté, *Adv. Mater.*, 2009, **21**, 697.
14 T. Kim, W. Lu, H. Lim, A. Han and Y. Qiao, *Appl. Phys. Lett.*, 2011, **98**, 053106.
15 M. L. Sha, D. X. Niu, Q. Dou, G. Z. Wu, H. P. Fang and J. Hu, *Soft Matter*, 2011, **7**, 4228.
16 F. Xia, H. Ge, Y. Hou, T. Sun, L. Chen, G. Zhang and L. Jiang, *Adv. Mater.*, 2007, **19**, 2520.
17 J. Zhang, X. Lu, W. Huang and Y. Han, *Macromol. Rapid Commun.*, 2005, **26**, 477.
18 D. Wu, S. Z. Wu, Q. D. Chen, Y. L. Zhang, J. Yao, X. Yao, L. G. Niu, J. N. Wang, L. Jiang and H. B. Sun, *Adv. Mater.*, 2011, **23**, 545.
19 D. Xia, X. He, Y. B. Jiang, G. P. Lopez and S. R. J. Brueck, *Langmuir*, 2010, **26**, 2700.
20 S. Z. Wu, D. Wu, J. Yao, Q. D. Chen, J. N. Wang, L. G. Niu, H. H. Fang and H. B. Sun, *Langmuir*, 2010, **26**, 12012.
21 D. Xia, L. M. Johnson and G. P. López, *Adv. Mater.*, 2012, **24**, 1287.
22 W. Xiong, Y. S. Zhou, X. N. He, Y. Gao, M. Mahjouri-Samani, L. Jiang, T. Baldacchini and Y. F. Lu, *Light: Sci. Appl.*, 2012, **1**, 1.
23 Y. L. Zhang, H. Xia, E. Kim and H. B. Sun, *Soft Matter*, 2012, **8**, 11217.
24 J. Y. Chung, J. P. Youngblood and C. M. Stafford, *Soft Matter*, 2007, **3**, 1163.
25 O. Bliznyuk, V. Veligura, E. S. Kooij, H. J. W. Zandvliet and B. Poelsema, *Phys. Rev. E: Stat., Nonlinear, Soft Matter Phys.*, 2011, **83**(4), 041607.
26 W. Li and A. Amirfazli, *Adv. Colloid Interface Sci.*, 2007, **132**, 51.
27 K. Ariga, T. Mori and J. P. Hill, *Adv. Mater.*, 2012, **24**, 158.

